ARCHIVES of FOUNDRY ENGINEERING

10.24425/afe.2026.157991

Published quarterly as the organ of the Foundry Commission of the Polish Academy of Sciences

ISSN (2299-2944)
Volume 2026
Issue 2/2026

72 – 82

8/2

Investigation of Fe and Mn Effects on the Fluidity Behavior of A356 Aluminum Alloys

M. Çolak [a], N. Alkan [b], Ü. Kutsal [c]

[a] Bayburt University, Vocational School of Technical Sciences, Türkiye
[b] Bayburt University, Graduate Education, Department of Mechanical Engineering, Türkiye
[c] Cevher Jant Sanayii A.Ş., Department of R&D, Türkiye
* Corresponding author: E-mail address: mcolak@bayburt.edu.tr

Received 30.10.2025; accepted in revised form 04.02.2026; available online 26.06.2026

Abstract

The fluidity behavior of Al–Si casting alloys is strongly influenced by impurity elements and intermetallic phase formation during solidification. In particular, iron (Fe) reduces melt fluidity by forming brittle Fe-rich intermetallics, whereas manganese (Mn) can mitigate this effect by modifying intermetallic morphology. In this study, secondary A356 aluminum alloys were produced with Fe contents of 0.10, 0.15, and 0.20 wt.% and nominal Mn additions of 0.05, 0.10, and 0.20 wt.% to investigate their combined effect on fluidity behavior. Melt quality was assessed using reduced pressure testing and density index measurements to ensure consistent casting conditions. Fluidity tests were conducted using spiral and eight-channel molds with section thicknesses ranging from 0.5 to 8 mm. To enable quantitative comparison across different section geometries, a Fluidity Index (FI) was defined based on section-normalized flow lengths. The results show that increasing Fe content generally reduces fluidity, while Mn additions significantly improve melt flow, with the most pronounced enhancement observed at 0.20 wt.% Mn. Thinner sections were found to be more sensitive to Fe-related flow restriction, whereas wider channels exhibited improved flow behavior. These findings demonstrate that appropriate Mn additions can effectively stabilize fluidity in secondary A356 alloys and provide practical guidelines for alloy control in recycled aluminum casting applications.

Keywords: A356 alloy, Castings defects, Fe impurity, Mn addition, Solidification process

1. Introduction

Aluminum alloys rank second among metallic materials after ferrous systems due to their low density, high specific strength, excellent corrosion and oxidation resistance, and versatility in manufacturing processes. Their use has expanded significantly in transportation, aerospace, and particularly in the automotive industry, where the demand for lightweight components continues to grow [1–4]. Secondary (recycled) aluminum production plays a vital role in meeting this demand by providing substantial energy savings and environmental benefits compared to primary production. However, several challenges are associated with the use of secondary aluminum, including the presence of impurities, inclusions, harmful intermetallics, and oxide films. Elements and compounds naturally occurring in aluminum, or introduced from scrap and alloying additions, are responsible for these defects [5]. The alloy composition thus becomes a key factor influencing product quality. Elements such as Fe, Cr, and Mn significantly affect the alloy's mechanical properties, fluidity, feeding, and castability by promoting inclusions, porosity, and oxide film formation [6]. Among these elements, iron is considered one of the most detrimental impurities determining the performance of aluminum casting alloys. Iron exhibits good solubility in the liquid phase of aluminum but very limited solubility in the solid state. Consequently, most of the iron present forms intermetallic compounds through bonding with other elements or impurities in the alloy. These Fe-rich intermetallics have negative effects on mechanical properties, porosity, corrosion resistance, and surface finish [7]. Increasing Fe content reduces ductility and fracture toughness while promoting brittle fracture behavior. Studies have shown that the critical Fe level strongly depends on the silicon content of the alloy. As the Si content increases, the tolerance for Fe before β-phase (β-Al_5FeSi) formation also increases. For example, the critical Fe level is approximately 0.35% for 5 wt% Si, 0.5% for 7 wt% Si, 0.6% for 9 wt% Si, and 0.75% for 11 wt% Si. Moreover, for a constant Fe level, the β-phase nucleation temperature decreases with increasing Si content [8]. Recent studies on recycled Al–Si–Mg alloys have emphasized that the Fe/Mn balance critically determines intermetallic morphology and mechanical performance [9].

Fluidity, the castability of an alloy, is defined as the distance that a liquid metal can flow in a mold cavity before solidification stops the movement. It is not an intrinsic material property such as density, but a process-dependent behavior governed by the interaction between liquid flow and solidification under specific casting conditions [10]. Therefore, fluidity must be evaluated through tests that account for temperature, alloy composition, and solidification rate, which are routinely performed in foundries. Numerous factors affect fluidity, generally categorized as metal-related and mold-related variables. These include alloy composition, pouring temperature, inclusions, oxides, bifilms, gating system design, viscosity, pouring time, cooling rate, and impurity content [11]. Several approaches are used to enhance fluidity, such as melt cleaning, increasing mold and casting temperatures, and adding inoculants [12]. Melt treatment aims to eliminate or minimize gas, inclusions, and residues that impede fluid flow; such undesirable effects can be effectively reduced through appropriate degassing and fluxing techniques [13]. Similarly, Mn additions have been reported to enhance melt flow and modify β-phase morphology, improving fluidity under both conventional and vacuum casting conditions [14].

Various alloying and impurity elements also influence the fluidity of aluminum melts. Additions of Fe, Zn, Cu, Mg, and Mn can markedly alter flow behavior. Increasing Fe content typically reduces fluidity due to enhanced intermetallic formation, whereas moderate additions of Mn can counteract this effect by modifying the Fe-bearing phases [15]. The relative concentration of these elements plays a decisive role: minor additions have little influence, while higher levels strongly affect the melt's viscosity and solidification dynamics. Mold and melt temperatures are also crucial. Lower mold temperatures shorten flow length by accelerating solidification, while preheating molds to about 200 °C or higher improves fluidity [16]. Likewise, fluidity increases with higher pouring temperatures for a given composition [17, 18]. Previous investigations on A413 and A356 alloys showed that Fe impurities reduce flow length, whereas Mn additions enhance it by transforming β-phase needles into more compact α-Al(FeMn)Si morphologies [19, 20]. The current work builds upon recent approaches redefining the Fluidity Index as a quantitative parameter linking melt cleanliness and flow performance [6].

In this study, the effects of Mn additions on the fluidity behavior of A356 alloys with varying Fe contents are systematically investigated. The work focuses on alloys produced from scrap materials to simulate secondary aluminum casting conditions. The influence of cross-sectional geometry and alloy composition on fluidity length is examined, and Fluidity Index (FI) values are determined as a function of Fe/Mn ratio and section thickness.

2. Experimental Procedure

In this study, the interaction of Mn with the characteristics of alloys containing different Fe levels was investigated. The Mn content was adjusted to 0.05%, 0.10%, and 0.20%, while the Fe content was varied at 0.10%, 0.15%, and 0.20%. Primary alloy, machining swarf, and recycled wheel scrap were used as raw materials. An Al–75 wt% Mn master alloy was employed to introduce Mn. Table 1 presents the chemical compositions of the alloys used in the experiments. The Fe content in the alloy was adjusted by adding machining swarf and primary alloy to the scrap rims. The melting process was conducted in an electric resistance furnace (10 kW power, 8 kg melt capacity) using a SiC crucible. The melt temperature was continuously monitored to ensure casting at the target temperature. When the melt reached 720 °C, the pre-calculated amount of Al75Mn master alloy was wrapped in aluminum foil, added to the melt, and manually stirred. Five minutes after Mn addition, rotary degassing was performed for 7 minutes using a gas flow rate of 7 l/min and an impeller speed of 350 rpm. When the melt temperature decreased to 700 °C, the crucible was removed from the furnace, and casting was carried out using three types of molds: a reduced pressure test (RPT) mold, an eight-channel fluidity mold, and a spiral fluidity mold. Prior to casting, both the spiral and eight-channel fluidity molds were coated with a refractory mold paint to ensure uniform surface conditions and to minimize metal–mold interaction. Before casting, all molds were preheated to 250 °C on a heating table to ensure thermal stability. The geometries of the eight-channel and spiral molds, with section thicknesses ranging from 0.5 mm to 8 mm, are shown in Figures 1 and 2, respectively. The width of the plate cavities in the eight-channel mold is constant and equal to 20 mm for all channels.

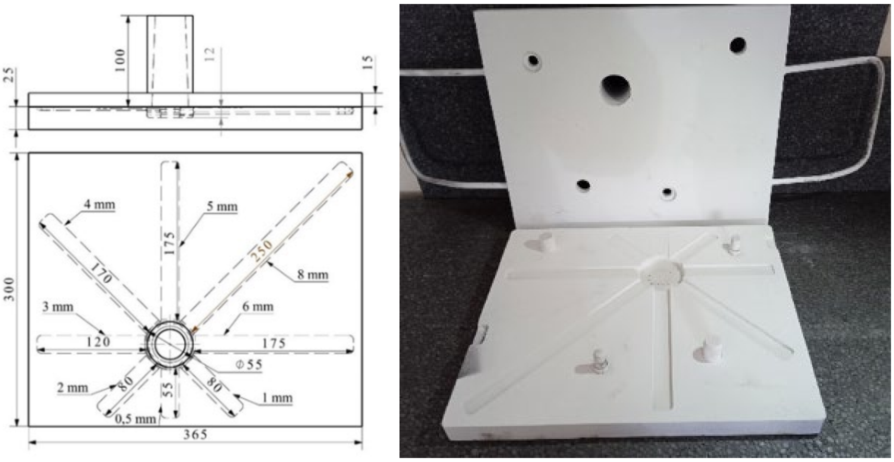

Fig. 1. 8-Channel Fluidity Pattern Dimensions and Pattern Image

After solidification and cooling, the castings were demolded to obtain RPT, eight-channel, and spiral samples. The samples were first examined macroscopically, and photographs were taken for documentation. The fluidity length was measured as the maximum length along each mold cavity where the molten metal completely filled and reproduced the cavity geometry. Measurements were taken from the ingate to the furthest point of complete mold filling in the selected cavity. The fluidity lengths were then measured for each section of the eight-channel mold. Because the mold features different section thicknesses, it can be difficult to directly compare flow lengths under varying casting conditions; therefore, each section was evaluated individually to account for possible variations.

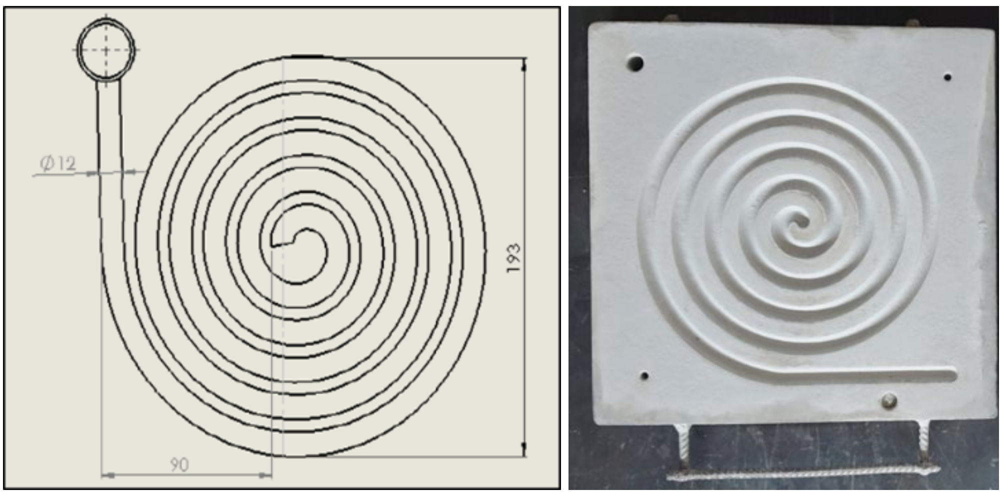

Fig. 2. Spiral Fluidity Mold Dimensions and Mold Image

The spiral fluidity length was defined as the maximum distance at which the molten metal completely filled and reproduced the spiral mold cavity geometry. Measurements were carried out along the apex (centerline) of the spiral channel using an image analysis method, with digital images calibrated by a reference scale to ensure measurement accuracy. To assess the repeatability of the measurements, the procedure was independently performed by different operators, and the consistency of the results confirmed the reproducibility of the method. Since the measured fluidity length can be influenced by several parameters, including pouring time, pouring temperature, the position of the ladle relative to the mold channels, and the pouring speed, a Fluidity Index (FI) was introduced to enable a standardized and quantitative comparison. This index is defined as the ratio between the liquid metal flow length in each channel and the corresponding section thickness. The total FI value is obtained by summing these ratios across all channels of the mold, thereby providing an average measure of melt fluidity under the given casting conditions. The mathematical expression of the Fluidity Index for the eight-channel mold is given in Equation (1):

$$FI = \Sigma (L_i / t_i) \quad (1)$$

where Li is the fluidity length measured in the i-th channel (mm), and ti is the corresponding section thickness of that channel (mm).

Since both parameters are expressed in millimeters, the resulting Fluidity Index (FI) is a dimensionless quantity. The Fluidity Index (FI) defined in Equation (1) is a dimensionless comparative parameter used to evaluate the cumulative flow performance of the molten alloy across multiple channel thicknesses. Higher FI values indicate improved overall fluidity under identical casting conditions. Although FI is not expressed as a filling percentage, it correlates with the overall filling ability of the plate-shaped cavities.

Density measurements of samples obtained from the RPT mold were performed based on Archimedes' principle. Each specimen was first weighed in air and then in distilled water using an Archimedes setup integrated with an analytical balance having a precision of ±0.02 g. The density index (DI) was calculated by comparing the densities of samples solidified under atmospheric and vacuum conditions, providing an indication of gas content and melt cleanliness. The Density Index (DI) was calculated using the following equation:

$$DI\ (\%) = [(\rho_{atm} - \rho_{vac}) / \rho_{atm}] \times 100$$

where ρ_{atm} is the density measured under atmospheric conditions and ρ_{vac} is the density measured under reduced pressure. To further examine internal porosity, the RPT specimens were sectioned vertically, and the cut surfaces were ground sequentially with 100- and 400-mesh sandpapers. The polished surfaces were then scanned at high resolution to digitally document the internal features for image analysis. This surface imaging was performed to qualitatively evaluate internal porosity and to visually support the Density Index results by confirming melt cleanliness, rather than to determine a quantitative bifilm index.

3. Results and Discussion

3.1. Determination of Chemical Composition Compatibility

The chemical composition results of the samples collected from the castings are summarized in Table 1. As indicated, all alloy compositions fall within the compositional limits of the A356 standard, and the targeted Fe and Mn additions were successfully achieved. In addition, both the experimental (setpoint) and actual Fe/Mn ratios are provided to allow a clearer assessment of compositional variations arising during melting and casting. Figure 3 compares the experimental and actual Fe/Mn ratios for all alloy conditions. Minor deviations between the setpoint and measured ratios are attributed to melting losses and compositional adjustments during alloy preparation; however, the overall trends are well preserved.

Table 1.
Chemical Composition Results of Casting (wt.%) and the experimental (Exp.) and actual (Act.) Fe/Mn ratio values.

Experiment	Si	Fe	Cu	Mn	Mg	Ti	Cr	Sr	Al	Fe/ Mn	
										Exp.	Act.
0.10 Fe-0.05 Mn	6.94	0.13	0.001	0.065	0.26	0.13	0.0010	0.003	92.46	2	2.00
0.10 Fe-0.10 Mn	7.35	0.12	0.003	0.102	0.22	0.12	0.0010	0.002	92.08	1	1.18
0.10 Fe-0.20 Mn	7.28	0.11	0.001	0.191	0.25	0.12	0.0008	0.035	92.01	0.5	0.58
0.15 Fe-0.05 Mn	7.18	0.17	0.001	0.046	0.24	0.13	0.0010	0.008	92.22	3	3.70
0.15 Fe-0.10 Mn	7.12	0.16	0.001	0.104	0.22	0.12	0.0010	0.003	92.26	1.5	1.54
0.15 Fe-0.20 Mn	7.38	0.17	0.001	0.202	0.25	0.13	0.0010	0.012	91.85	0.75	0.84
0.20 Fe-0.05 Mn	7.31	0.21	0.004	0.058	0.29	0.12	0.0031	0.008	91.98	4	3.62
0.20 Fe-0.10 Mn	7.33	0.19	0.001	0.112	0.21	0.12	0.0009	0.002	92.03	2	1.70
0.20 Fe-0.20 Mn	7.27	0.19	0.001	0.201	0.20	0.13	0.0008	0.001	92.21	1	0.95

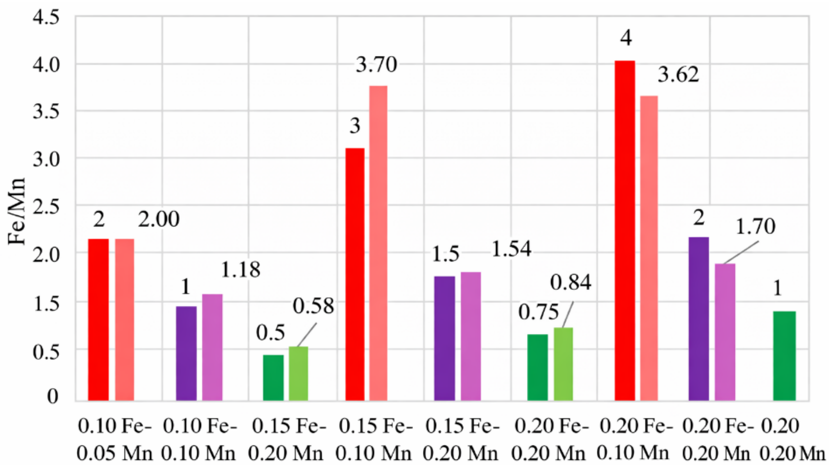

Fig. 3. Fe/Mn ratios for the setpoint values used in the experiment and the actual values obtained (Experimental values; left, actual values right)

The roles of Fe and Mn are particularly critical in governing the melt fluidity behavior of the investigated alloys. Due to its limited solid solubility in aluminum, Fe tends to form β-Al_5FeSi intermetallic phases with a needle-like morphology, which obstruct liquid metal flow within the mold and adversely affect fluidity [8, 20]. In contrast, Mn additions promote the transformation of these detrimental β-phases into more compact and less harmful α-Al(FeMn)Si intermetallics. This β-to-α phase modification mechanism reduces flow obstruction and facilitates melt advancement, thereby improving fluidity. Similar effects of Mn on modifying Fe-rich intermetallics and enhancing both fluidity and mechanical integrity in Al–Si–Mg alloys have been widely reported in the literature [6, 18].

3.2. Analysis of Liquid Metal Quality

In this study, melt quality tests were performed prior to casting to prevent the influence of entrapped or dissolved gases on the experimental results. The liquid metal quality was evaluated using samples solidified in the Reduced Pressure Test (RPT) mold. Density measurements were performed on the solidified samples to assess gas porosity and melt cleanliness. Figure 4 presents the average density index values obtained from the experiments. The density index values ranged from 0.29 to 0.85, as shown in Figure 4. The lowest value of 0.29 was obtained for the alloy containing 0.15 wt.% Fe – 0.10 wt.% Mn, while the highest value of 0.85 corresponded to the 0.10 wt.% Fe – 0.20 wt.% Mn composition. Density index values between 0.29 and 0.85 indicate that the melt quality is within the acceptable cleanliness range for aluminum alloys. A low-density index signifies a smaller amount of gas and inclusions in the melt, which positively affects the fluidity performance. Literature reports that lower density index values correspond to reduced bifilm and gas content, leading to longer fluidity distances [21–23]. Consistent with these findings, in the present study, the alloys exhibiting lower density indices also showed greater liquid metal flow lengths, confirming the effectiveness of the melt cleaning process. The RPT samples solidified under vacuum were sectioned vertically to examine their internal porosity. The sectioned surfaces were ground and scanned for macrostructural evaluation. The resulting scanned images of the cross-sections are presented in Figure 5.

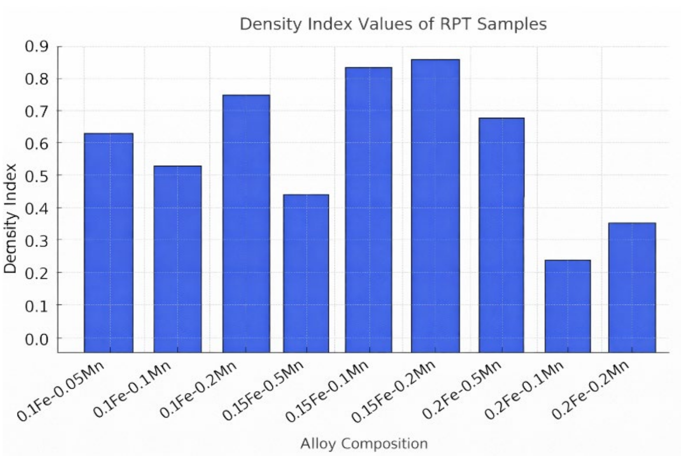

Fig. 4. Density Index Values

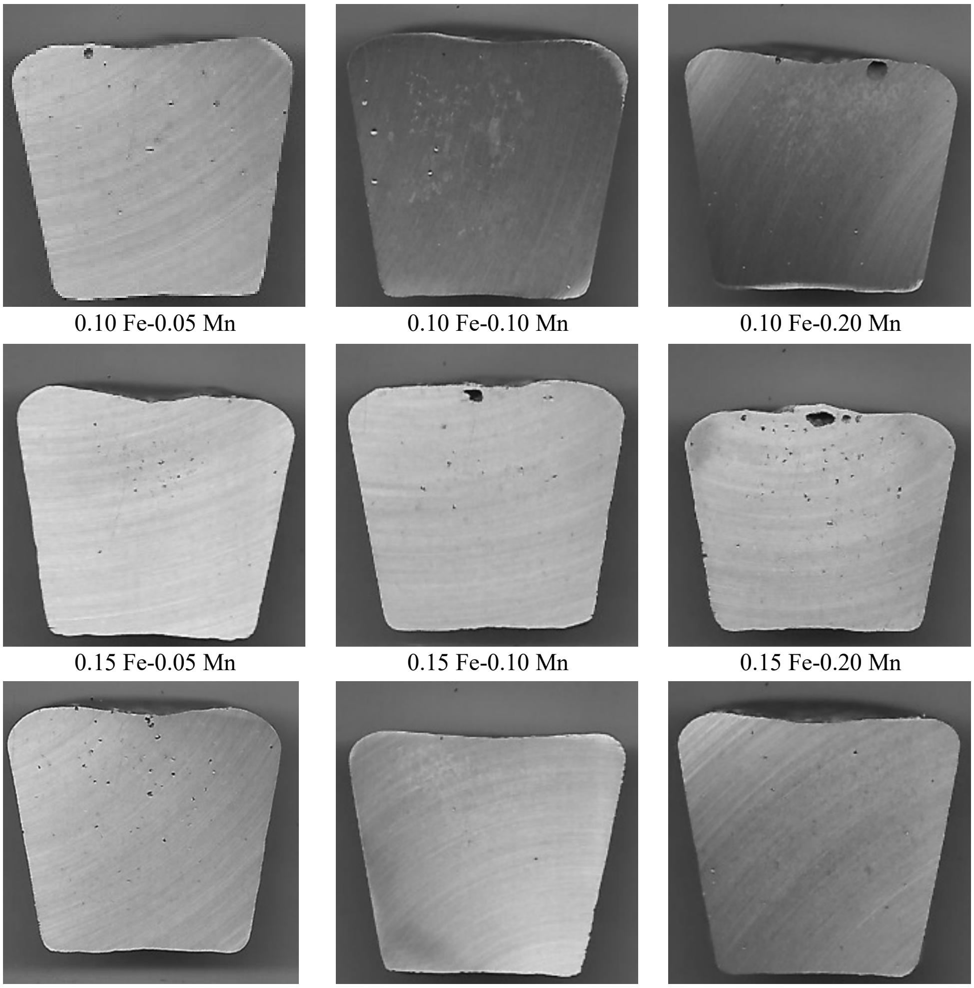

0.10 Fe-0.05 Mn | 0.10 Fe-0.10 Mn | 0.10 Fe-0.20 Mn
0.15 Fe-0.05 Mn | 0.15 Fe-0.10 Mn | 0.15 Fe-0.20 Mn
0.20 Fe-0.05 Mn | 0.20 Fe-0.10 Mn | 0.20 Fe-0.20 Mn

Fig. 5. Cross-Sectional Surface Images of RPT Samples

When the cross-sectional surfaces in Figure 5 are examined, minimal surface porosity further supports the high cleanliness of the melt. Although some isolated large and small pores are visible on the scanned RPT surfaces, the Density Index (DI) represents an overall measure of melt gas content rather than the complete absence of localized porosity. The relatively low DI values indicate effective hydrogen removal, while the observed pores are mainly attributed to localized solidification and shrinkage effects. Several researchers have reported that the presence of shallow surface depressions and the absence of visible porosity in RPT samples indicate acceptable melt quality [21, 22]. Similarly, in a separate study, it was determined that a porosity level below 0.5% and the presence of smooth surface depressions correspond to clean melt conditions suitable for casting [23].

3.3. Fluidity Test Results

The parameters influencing the fluidity behavior of the A356 aluminum alloy during casting were investigated using both spiral and eight-channel fluidity molds. Representative samples obtained from castings performed in the spiral fluidity mold under different experimental conditions are presented in Figure 6. The corresponding average liquid metal flow lengths derived from these samples are illustrated in Figure 7. In addition, representative samples obtained from the eight-channel fluidity mold are shown in Figure 8 for comparison.

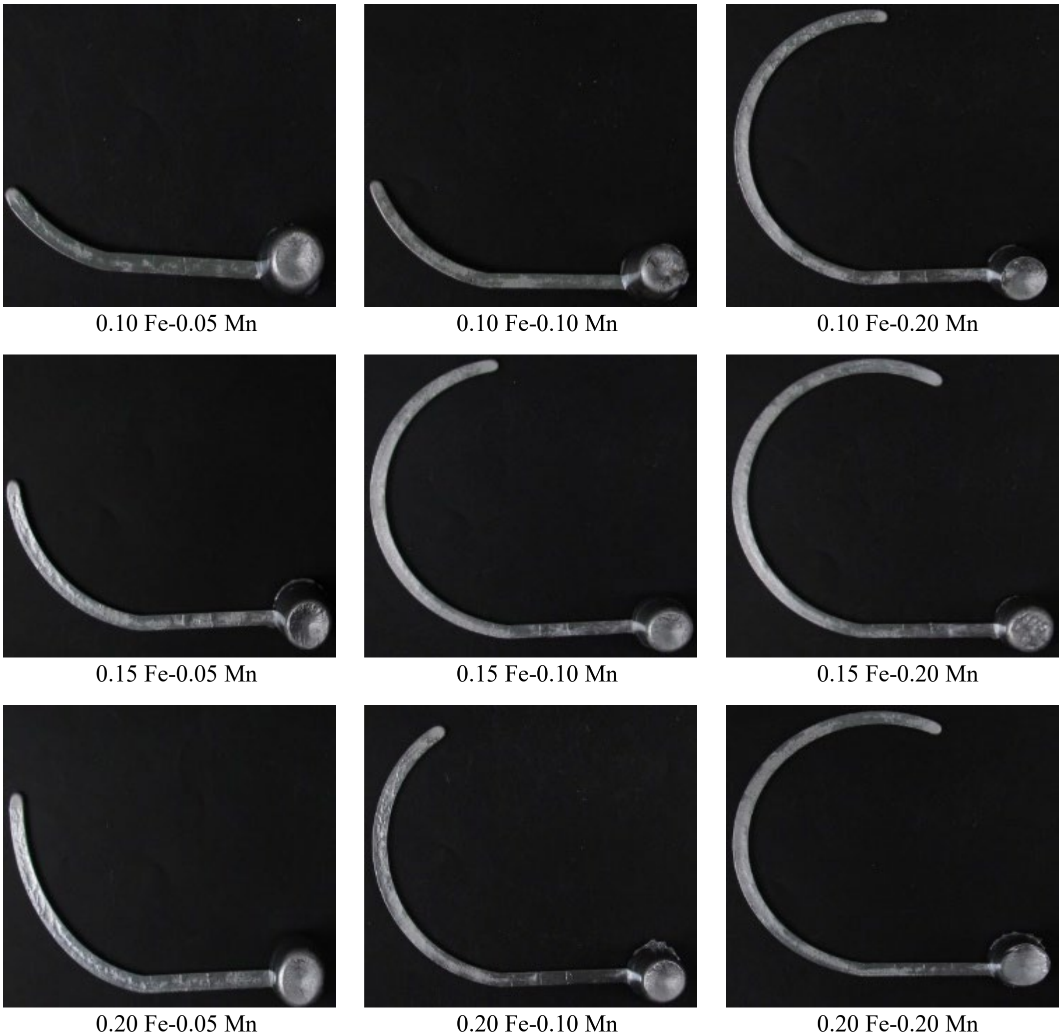

Fig. 6. Spiral Fluidity Sample Images

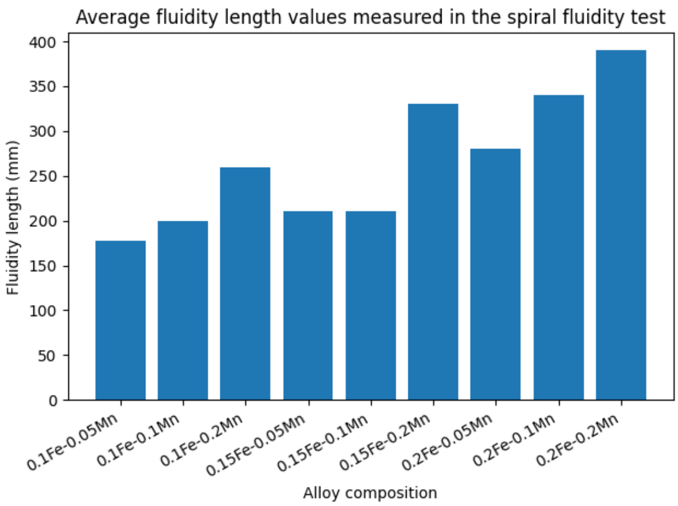

Fig. 7. Spiral Fluidity Length Results

When the spiral fluidity samples shown in Figure 6 and the eight-channel fluidity samples presented in Figure 8 are examined, it is evident that the liquid metal flow lengths vary with changes in the experimental parameters. As illustrated in Figure 7, the fluidity length ranged from 178 mm to 394 mm. The highest flow length, 394 mm, was obtained for the alloy containing 0.2 wt.% Fe and 0.2 wt.% Mn, whereas the lowest, 178 mm, was measured for the alloy with 0.1 wt.% Fe and 0.05 wt.% Mn. Within the investigated composition range and in the presence of Mn, an apparent increase in flow length was observed with rising Fe content. These findings indicate that both Fe and Mn contents have a positive influence on melt flow behavior within the tested composition range.

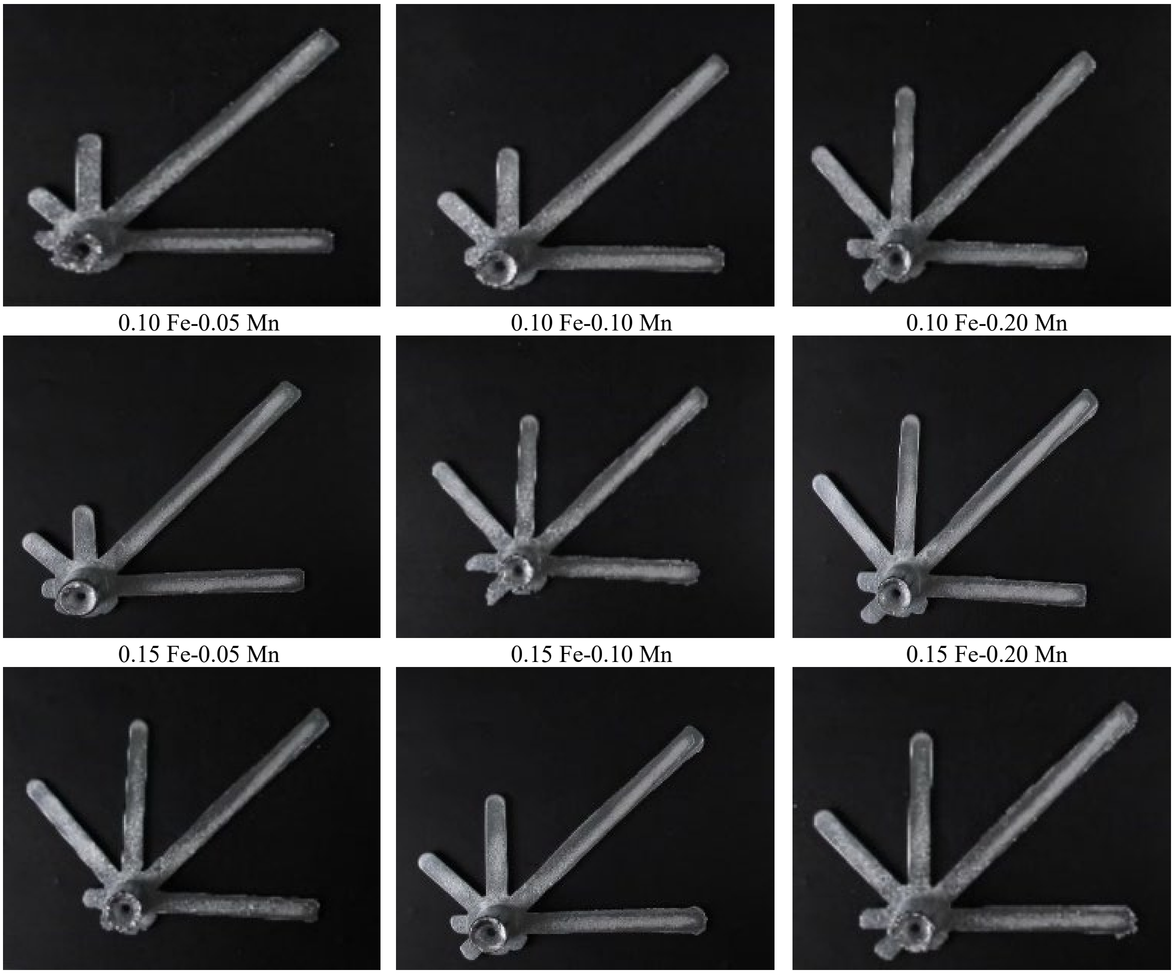

0.10 Fe-0.05 Mn | 0.10 Fe-0.10 Mn | 0.10 Fe-0.20 Mn

0.15 Fe-0.05 Mn | 0.15 Fe-0.10 Mn | 0.15 Fe-0.20 Mn

0.20 Fe-0.05 Mn | 0.20 Fe-0.10 Mn | 0.20 Fe-0.20 Mn

Fig. 8. 8-Channel Fluidity Samples

The average fluidity length distances obtained from the eight-channel fluidity tests are summarized in Table 2. Figure 9 presents the fluidity characteristics of the eight-channel plate mold, showing the variation of fluidity length (L_i) with section thickness (t_i) for different Mn contents at constant Fe levels. At a constant Fe content, increasing Mn content from 0.05 to 0.20 wt.% generally led to higher fluidity lengths, particularly in thinner sections. In addition, the fluidity length increased with increasing section thickness (t_i) for all alloy compositions; however, a tendency toward saturation was observed in the thicker channels, indicating geometric limitations of the mold.

Table 2.
8-Channel Fluidity Length Results

	Fluidity Length **(mm)**								
	0.5	**1**	**2**	**3**	**4**	**5**	**6**	**8**	**Fluidity Index (FI)**
0.10 Fe-0.05 Mn	4	9	8	11	45	52	175	250	106.73
0.10 Fe-0.10 Mn	4	8	7	15	62	83	175	250	117.02
0.10 Fe-0.20 Mn	8	9	14	28	46	97	175	250	132.65
0.15 Fe-0.05 Mn	7	9	18	10	57	75	175	250	125.00
0.15 Fe-0.10 Mn	8	10	19	21	95	125	175	250	151.67
0.15 Fe-0.20 Mn	8	9	11	20	126	148	175	250	158.68
0.20 Fe-0.05 Mn	7	9	27	19	17	132	175	250	133.90
0.20 Fe-0.10 Mn	5	9	23	24	104	140	175	250	152.92
0.20 Fe-0.20 Mn	8	11	32	35	114	129	175	250	169.38

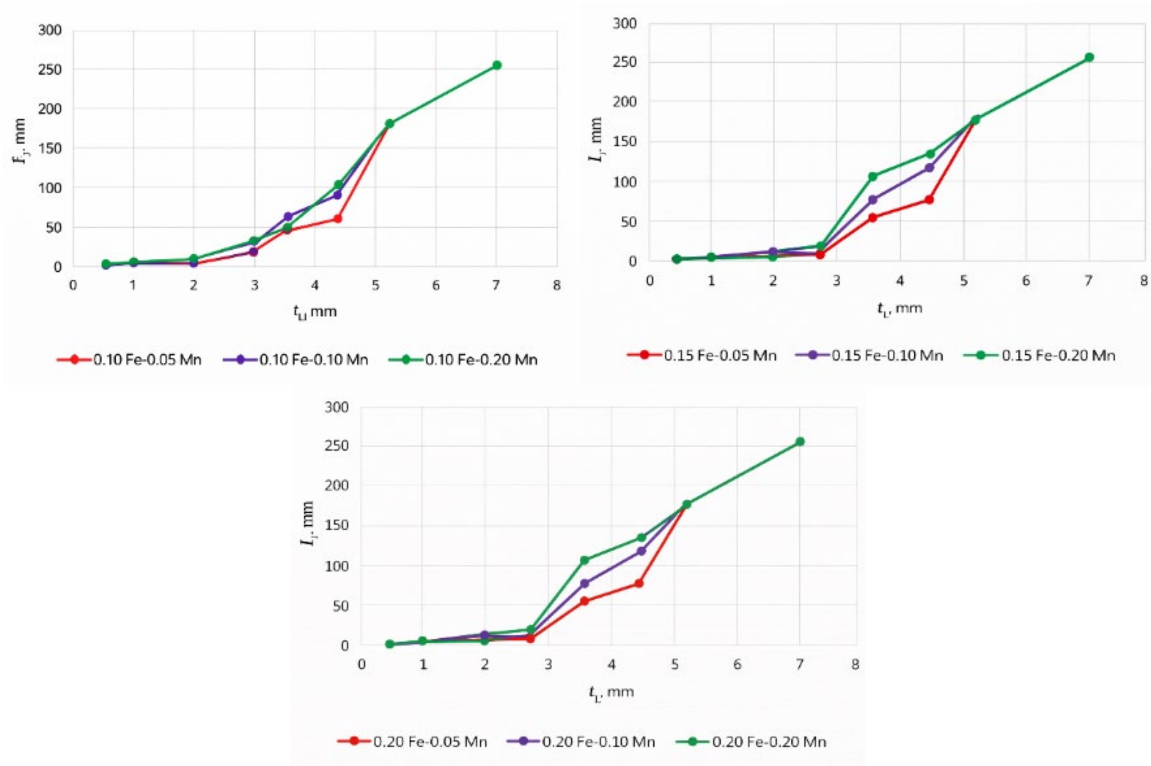

Fig. 9. Fluidity characteristics of alloy A356 for Mn contents of approx. 0.05 wt.%, 0.10 wt.% and 0.20 wt.% and Fe contents in the alloy of approx.: a)0.10 wt.%, b) 0.15 wt.%, c) 0.20 wt.%

Examination of the results presented in Table 2 reveals that the liquid metal flow length varies with section thickness and alloy composition. Overall, fluidity increased with the simultaneous rise in Fe and Mn contents. Although Fe is generally regarded as a detrimental impurity in aluminum alloys due to its tendency to form brittle intermetallics, the present findings demonstrate that its adverse effects can be effectively mitigated—and even reversed—through the addition of Mn. In the multi-channel fluidity test, the fluidity length increased with increasing channel thickness and reached a maximum limit in the 6 mm and 8 mm channels due to the physical constraints imposed by the mold geometry. This saturation behavior in the 6 mm and 8 mm channels is attributed to geometric limitations of the mold, which may reduce the sensitivity of the fluidity index for highly fluid alloys in thicker sections. Nevertheless, the fluidity index remains effective for comparative evaluation of alloy composition effects across different section thicknesses. The fluidity index approach proved to be an effective method for comparing molds with different cross-sectional geometries and for quantifying the influence of compositional variations on melt behavior [6]. In the A356 alloys examined, increasing Mn content in the presence of Fe led to improved melt flow distances, with the highest flow length of approximately 394 mm recorded in the spiral mold containing 0.2 wt.% Fe and 0.2 wt.% Mn. The spiral mold results reflected the unidirectional advancement of the molten metal, while the eight-channel mold enabled assessment of flow behavior across multiple section thicknesses. Fluidity limitations were, as expected, more pronounced in the thinnest channels, but alloys with higher Fe and Mn levels exhibited overall greater fluidity. Although Fe is generally considered detrimental to the mechanical properties of aluminum alloys due to the formation of brittle intermetallic phases, the present results indicate that its negative influence on fluidity can be effectively mitigated by Mn additions. As shown in Table 2, increasing Mn content at a given Fe level leads to higher fluidity length and fluidity index values, confirming the role of Mn in modifying Fe-rich intermetallic morphology. This indicates that the Fe–Mn interaction, rather than Fe content alone, governs the flowability in these alloys. From a metallurgical standpoint, this improvement is attributed to the solidification mechanism in which Fe promotes the formation of needle-shaped β-Al_5FeSi intermetallics that tend to obstruct liquid metal flow. However, when Fe is accompanied by Mn, these β-phases transform into the more compact and less harmful α-Al(FeMn)Si morphology, which facilitates melt advancement within the mold [8, 10]. This synergistic effect between Fe and Mn explains the increase in fluidity observed at higher combined concentrations of these elements. The transformation also contributes to better phase distribution and reduced risk of flow blockage, particularly in alloys cast from recycled feedstock.

Complementary to alloy chemistry, melt cleaning processes—such as rotary degassing and filtration—play a vital role in minimizing oxide films, bifilms, and gas porosity in the melt. These treatments enhance the overall cleanliness of the liquid metal, thereby stabilizing the flow characteristics and improving the reproducibility of fluidity measurements [24, 25]. In summary, both experimental findings and literature evidence indicate that maintaining an optimized Fe/Mn ratio in secondary A356 melts promotes the formation of favorable α-phase structures, enhances fluidity, and mitigates the negative impact of Fe impurities. This approach provides a practical pathway for improving casting performance while supporting the recyclability and sustainability of aluminum alloy production. The Fluidity Index (FI) defined in Equation (1) is a dimensionless comparative parameter used to evaluate the cumulative flow performance of the molten alloy across multiple channel thicknesses. Higher FI values indicate improved overall fluidity under identical casting conditions and correlate with the overall filling ability of the plate-shaped cavities. Due to the limited number of experimental conditions, the dependence of FI on alloy composition parameters was evaluated through trend analysis and graphical interpretation rather than full regression-based statistical modeling.

4. Conclusion

In this study, the effects of different Fe and Mn ratios on the fluidity properties of the A356 aluminum alloy were systematically investigated. The key findings are summarized below:

- The chemical composition analyses confirmed compliance with the A356 standard, and the targeted Fe and Mn ratios were successfully achieved.
- Liquid metal cleanliness was verified through RPT tests and density measurements, revealing low porosity levels and demonstrating that the melt-cleaning processes were effective.
- In the spiral mold tests, the liquid metal flow lengths ranged between 178 mm and 394 mm. The highest flow length (394 mm) was obtained for the 0.2 wt.% Fe–0.2 wt.% Mn composition, while the lowest (178 mm) was recorded for 0.1 wt.% Fe–0.05 wt.% Mn.
- In the castings made using the eight-channel fluidity mold, variations in flow distance were observed depending on the section thickness. When the flow index values were compared with those from the spiral mold, the results were consistent, showing that fluidity increased with the combined rise of Fe and Mn contents.
- The fluidity index approach allowed reliable comparisons across varying section thicknesses and produced results consistent with the literature.
- Among all compositions, the most significant improvement in fluidity was achieved at 0.2 wt.% Mn.
- In addition, the Density Index (DI) results confirmed that the melt quality was within an acceptable cleanliness range for all alloy conditions. Lower DI values, indicating reduced gas and bifilm content, were associated with higher fluidity index (FI) values, demonstrating that improved melt cleanliness positively contributed to the observed enhancement in fluidity behavior.

Mn additions improve the fluidity behavior of A356 aluminum alloys by modifying Fe-rich intermetallic phases; under appropriate Al–Fe–Mn combinations, the interaction between Fe and Mn governs the melt flow behavior rather than Fe content alone. The optimum composition was identified as 0.2 wt.% Mn, particularly when accompanied by moderate Fe levels. These findings provide a practical approach to enhancing casting quality, especially in secondary aluminum production processes used in the automotive industry.

Acknowledgement

The authors would like to express their sincere gratitude to Cevher Jant Sanayii A.Ş. for their valuable support in the realization of this study.

References

[1] Rooy, E.L. (1990). Introduction to aluminum and aluminum alloys. In *Properties and selection: nonferrous alloys and special-purpose materials* (pp. 3–14). Materials Park, OH: ASM International. https://doi.org/10.31399/asm.hb.v02.a0001057.

[2] Vatansever, F., Ertürk, A.T. & Karabay, S. (2018). Improvement of the microstructural and mechanical properties of aluminum–silicon alloys by T6 heat treatment. *Dokuz Eylul University Journal of Engineering and Science.* 20(60), 797-803 (in Turkish).

[3] Chen, W.F. & Lui, E.M. (2005). *Handbook of structural engineering*. Boca Raton, FL: CRC Press.

[4] Yagci, T., Cocen, U., Culha, O. & Korkmaz, A. (2021). A general review and evaluation of recent academic and industrial developments in aluminum casting alloys. *Uludag University Journal of Engineering Faculty*. 26(3), 1191-1210 (in Turkish).

[5] Dispinar, D. (2006). *Determination of metal quality of aluminium and its alloys*. Doctoral dissertation, University of Birmingham, Birmingham, United Kingdom.

[6] Durmus, M., Dispinar, D., Gavgali, M., Uslu, E. & Colak, M. (2025). Evaluation of Fe content on the fluidity of A356 aluminum alloy by a new fluidity index. *International Journal of Metalcasting*. 19(3), 1590-1604. https://doi.org/10.1007/s40962-024-01396-4.

[7] Ak, M. (2012). *Investigation of the effects of iron impurity on the mechanical properties of AA206 aluminum casting alloy*. Thesis (in Turkish).

[8] Taylor, J.A. (2012). Iron-containing intermetallic phases in Al–Si based casting alloys. *Procedia Materials Science*. 1, 19-33. DOI: 10.1016/j.mspro.2012.06.004.

[9] Huang, Y., Li, L., Wen, J. & Liu, Y. (2024). Evolution behavior of Fe and Fe-rich phases in high-Fe concentration Al–Si–Mg alloy alloyed with Mn, Cr, and Co. *Materials Today Communications*. 39, 108753, 1-12. https://doi.org/10.1016/j.mtcomm.2024.108753.

[10] Di Sabatino, M. & Arnberg, L. (2004). A review on the fluidity of Al-based alloys. *Metallurgical Science and Technology*. 22(1), 9-15.

[11] Fazeli, A.H., Saghafian, H., Boutorabi, S.M.A. & Campbell, J. (2022). The fluidity of aluminium ductile irons. *International Journal of Metalcasting*. 16(1), 143-152. https://doi.org/10.1007/s40962-021-00581-z.

[12] Asan, Y.E. & Colak, M. (2022). Modeling the effect of pour height, casting temperature and die preheating temperature on the fluidity of different section thicknesses in permanent mold casting of Al12Si alloys. *Erzincan University Journal of Science and Technology*. 15(Spec.I), 14-27. https://doi.org/10.18185/erzifbed.1199648.

[13] Tokatli, M., Saydam, F., Hal, M., Kosatepe, A., Colak, M. & Yuksel, C. (2022). Investigation of commonly used liquid metal cleaning methods in the casting of aluminum alloys. *Journal of the Institute of Science and Technology*. 12(1), 423-434 (in Turkish).

[14] Callegari, B., Lima, T.N. & Coelho, R.S. (2023). The influence of alloying elements on the microstructure and properties of Al–Si-based casting alloys: A review. *Metals*. 1(7), 1174, 1-36. https://doi.org/10.3390/met13071174.

[15] Obara, T.J., Minei, R.O., Kakitani, R., Spinelli, J.E., Garcia, A. & Cheung, N. (2023). Solidification microstructure and mechanical properties of an Al–11 wt.% Si alloy modified with Nb and Sb. *Journal of Physics and Chemistry of Solids*. 181, 111521, 1-10. DOI: 10.1016/j.jpcs.2023.111521.

[16] Ravi, K.R., Pillai, R.M., Amaranathan, K.R., Pai, B.C. & Chakraborty, M. (2008). Fluidity of aluminum alloys and composites: A review. *Journal of Alloys and Compounds*. 456(1-2), 201-210. https://doi.org/10.1016/j.jallcom.2007.02.038.

[17] Han-Hua, W., Zeng-Sun, J., Bei-Yu, L., Feng-Rong, Y. & Xian-Yi, L. (2003). Characterization of the microarc oxidation process on aluminium alloy. *Chinese Physics Letters*. 20(10), 1815-1818. DOI: 10.1088/0256-307X/20/10/345.

[18] Prukkanon, W., Srisukhumbowornchai, N. & Limmaneevichitr, C. (2009). Influence of Sc modification on the fluidity of an A356 aluminum alloy. *Journal of Alloys and Compounds*. 487(1-2), 453-457. https://doi.org/10.1016/j.jallcom.2009.07.169.

[19] Haga, T., Imamura, S. & Fuse, H. (2021). Fluidity investigation of pure Al and Al–Si alloys. *Materials*. 14(18), 5372, 1-15. https://doi.org/10.3390/ma14185372.

[20] Taghaddos, E., Hejazi, M.M., Taghiabadi, R. & Shabestari, S. G. (2009). Effect of iron intermetallics on the fluidity of 413 aluminum alloy. *Journal of Alloys and Compounds*. 468(1-2), 539-545. https://doi.org/10.1016/j.jallcom.2008.01.079.

[21] Dispinar, D., Akhtar, S., Nordmark, A., Di Sabatino, M. & Arnberg, L. (2010). Degassing, hydrogen and porosity phenomena in A356. *Materials Science and Engineering: A*. 527(16-17), 3719-3725. https://doi.org/10.1016/j.msea.2010.01.088.

[22] Yuksel, C. (2016). *Improvement of liquid metal quality of aluminum and its alloys*. Doctoral dissertation, Yildiz Technical University, Istanbul, Türkiye (in Turkish).

[23] Uludag, M., Cetin, R., Dispinar, D. & Tiryakioglu, M. (2018). On the interpretation of melt quality assessment of A356 aluminum alloy by the reduced pressure test: The bifilm index and its physical meaning. *International Journal of Metalcasting*. 12(4), 853-860. https://doi.org/10.1007/s40962-018-0217-4.

[24] Erzi, E., Gursoy, O., Yuksel, C., Colak, M. & Dispinar, D. (2019). Determination of acceptable quality limit for casting of A356 aluminium alloy: Supplier's quality index (SQI). *Metals*. 9(9), 957, 1-14. https://doi.org/10.3390/met9090957.

[25] Colak, M., Kayikci, R. & Dispinar, D. (2016). Melt cleanliness comparison of chlorine fluxing and Ar degassing of secondary Al–4Cu. *Metallurgical and Materials Transactions B*. 47(5), 2705-2709. https://doi.org/10.1007/s11663-016-0745-3.